

# A double layer nanostructure SiC coating for anti-oxidation protection of carbon/carbon composites prepared by chemical vapor reaction and chemical vapor deposition

Xin Yang<sup>a,b</sup>, Qizhong Huang<sup>a,\*</sup>, Zhean Su<sup>a</sup>, Liyuan Chai<sup>b</sup>, Xiufei Wang<sup>a</sup>, Leping Zhou<sup>a</sup>

<sup>a</sup>State Key Laboratory of Powder Metallurgy, Central South University, Changsha 410083, PR China

<sup>b</sup>School of Metallurgical Science and Engineering, Central South University, Changsha 410083, PR China

Received 15 October 2012; received in revised form 29 November 2012; accepted 30 November 2012

Available online 10 December 2012

## Abstract

A double layer nanostructure SiC coating was prepared by chemical vapor reaction and chemical vapor deposition to protect carbon/carbon composites from oxidation. The obtained dense coating reveals a typical crystalline structure and combines well with the substrate. The outer layer of the coating consists of SiC nanocrystals and nanowires, whereas the inner layer is mainly composed of SiC microcrystals, nanocrystals and nanowires. The oxidation and cyclic thermal shock test performed at 1400 °C in air demonstrates that the prepared dense nanostructure coating has excellent anti-oxidation behavior and thermal shock resistance at high temperature. After 400 h oxidation and 34 cycles of thermal shock from 1400 °C to room temperature, the weight loss of the coated sample is only 1.67%. In the oxidation process, the amorphous silica formed at the beginning of the oxidation crystallizes to cristobalite as oxidation time increased. The formation of cristobalite resulted in micro-cracks formed along grain boundaries in the cyclic thermal shock test. As only cracks are formed on the coating surface, it can be concluded that the formation of the penetration cracks may be the reason for the weight loss of the SiC coated composite.

Crown Copyright © 2012 Published by Elsevier Ltd and Techna Group S.r.l. All rights reserved.

**Keywords:** D. SiC; Oxidation resistance; Coating; Carbon/carbon composites

## 1. Introduction

Carbon/carbon (C/C) composites have attracted much attention for high temperature structural applications due to their excellent properties of lightweight, high strength, high thermal stability and resistance to ablation [1]. However, their susceptibility to oxidation above 500 °C limits their extensive applications as high temperature structural materials [2]. Therefore, the technology of reliable oxidation protection is crucial to exert their full potential. To solve this problem, much effort has been carried out to explore new coating technologies and anti-oxidation coating systems, and it is generally acknowledged that SiC is one of the most

ideal coating materials for C/C composites due to its good mechanical properties, excellent anti-oxidation property and good physical–chemical compatibility with carbon materials [3,4]. Up to now, SiC coating can be formed on C/C composites by several methods such as pack cementation [5], chemical vapor deposition (CVD) [6,7], laser-induced chemical decomposition (LICD) [8], reactive infiltration [9], slurry-sintering [10] and plasma spraying technology [11]. However, it is difficult to obtain a dense structure from a single layer coating using these methods. Usually, the defects such as pores and cracks formed in the coating during preparation or cooling stage will inevitably affect their anti-oxidation property. To further improve their anti-oxidation property, SiC dense coatings with multi-layers or multi-phase composition are proposed and achieve partial success [1–3,12–18]. Though the oxidation resistance of these dense SiC coatings are greatly improved, however, as the coating and carbon substrate are two different materials, the mismatch

\*Corresponding author. Tel.: +86 731 88836078;  
fax: +86 731 88877671.

E-mail addresses: [qzhuang@csu.edu.cn](mailto:qzhuang@csu.edu.cn),  
[qizhonghuangcsu@yahoo.cn](mailto:qizhonghuangcsu@yahoo.cn) (Q.Z. Huang).

of the thermal expansion coefficient (CTE) will induce internal stress between them. Therefore, when they serve in the severe environment with cyclic thermal shock load, the cracking or debonding of the coating will result in the protection failure. In this condition, the design of functionally graded coatings [19–21] and nanowire (or whisker) toughened coatings [22–25] are feasible ways to extend their service life. As the composition of the functionally graded coatings changes gradually from inner substrate to outer coating surface, the continuous distribution of the Young's modulus and the CTE of the coating materials can effectively relax the thermal mismatch between them, consequently, the thermal shock resistance of this coating can be improved greatly. However, the accurate control of the composition and microstructure of the graded coatings is a significant challenge. Recent studies demonstrate that addition of nanowires into SiC coating is also an effective way to improve their thermal shock resistance [26,27], and the reported research has shown that the nanowire toughened SiC coatings exhibited excellent oxidation and thermal shock resistance at high temperature. In the previous work, Chu

et al. [26] prepared an oxidation protective Si–SiC coating with SiC nanowires by a two-step technique. First, a SiC inner coating was coated on C/C composites by pack cementation, and then SiC nanowires were produced on the inner coating by exposure to the vapors from heating a powder of mixed Si+SiO<sub>2</sub>. Finally, the obtained nanowire coating was infiltrated by pack cementation. However, the further infiltration process of the nanowire coating at high temperature may damage SiC nanowires and results in degradation of their mechanical properties. In addition, another method by Qiang et al. [27] introduced SiC nanowires on SiC inner layer by pack cementation with ferrocene as catalyst. Afterwards, a CVD SiC outer layer was deposited on the prepared coating surface. In the coating process, Fe was inevitably formed due to the decomposition of ferrocene catalyst, which is unfavorable for the anti-oxidation property of the coating.

As is well known, CVD is a mature technology that can provide highly pure materials with structural control at atomic or nanometer scale level. Moreover, it can produce single layer, multilayer, composite, nanostructured, and

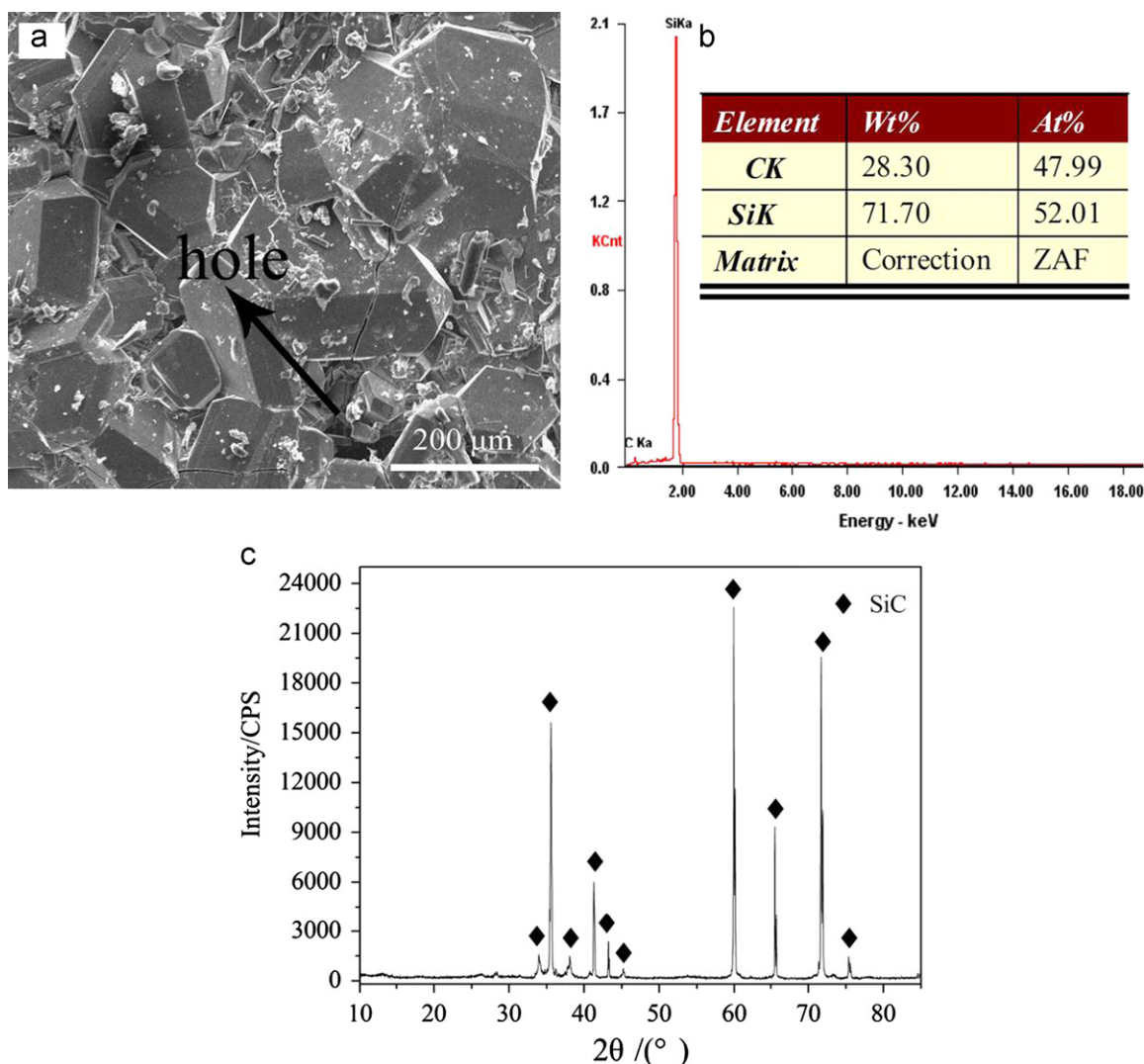


Fig. 1. Surface morphology, EDS and XRD analyses of the CVR SiC coating prepared on C/C composites.

functionally graded coating materials with well controlled dimension and unique structure at low processing temperatures [28]. According to the reported research, SiC nanowires (or whiskers) are successfully synthesized by this method [29–31]. Compared with the above two methods to prepare SiC nanowires, this method is high reliable, well repeatable and less damage to nanowires due to the relative low deposition temperature. In the present study, we report a double layer nanostructure SiC coating toughened with SiC nanowires produced by chemical vapor reaction (CVR) and CVD. Firstly, the SiC inner coating was prepared by CVR, and then the CVD SiC coating was deposited as outer layer. In the CVD process, SiC nanowires and nanoparticles were successfully introduced into CVR inner layer and CVD outer layer. The microstructure of this special dense coating was examined and also the oxidation behavior and thermal shock resistance of the coated sample were investigated. It is believed that the report of our new work may offer an effective way to improve the oxidation property and thermal shock resistance of the SiC coated C/C composites that applied in severe condition.

## 2. Experimental

The double layer nanostructure SiC coating toughened with SiC nanowires were prepared by the following steps: firstly, the pre-coated C/C composites with density of  $1.81 \text{ g/cm}^3$  were cut into small specimens and then hand-polished with 600 grit SiC paper. After a clean and thorough drying process, the samples were placed in a graphite crucible. Si sheets (industrial reagent,  $>99.4\%$ ) and  $\text{SiO}_2$  powders (industrial reagent,  $>99.2\%$ ) were used as starting materials for CVR. Before the CVR, the mixed Si sheets and  $\text{SiO}_2$  powders were put at the bottom of the graphite crucible. When heated at high temperature ( $>1600^\circ\text{C}$ ), SiO vapor generated via the reaction of Si and  $\text{SiO}_2$  will react with carbon substrate to form the SiC coating [32,33]. The whole CVR process was conducted at the temperature within the range of  $1800\text{--}2100^\circ\text{C}$  for 1–3 h, followed by a natural cooling course. Secondly, a CVD SiC coating was deposited on the CVR SiC coated samples by using methyltrichlorosilane (MTS).  $\text{H}_2$  was used as the carrier gas and Ar was used as the diluent gas. The deposition of SiC outer layer was performed at temperature of  $1100^\circ\text{C}$  with a total pressure of 5 kPa. The flow rates of  $\text{H}_2$ , MTS and Ar

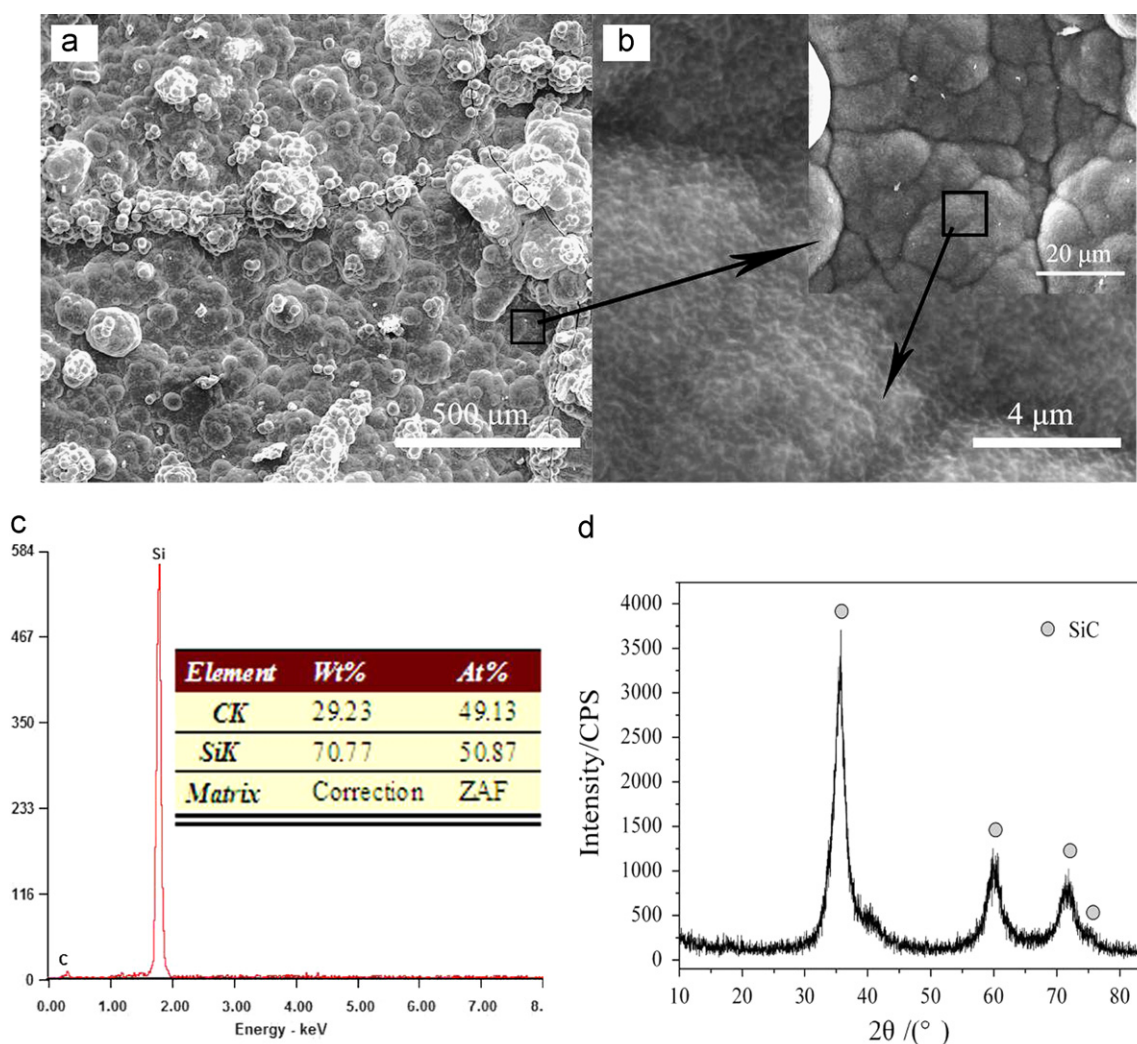


Fig. 2. SEM images, EDS and XRD analyses of the outer layer CVD SiC coating.



were  $300 \text{ mL min}^{-1}$ ,  $300 \text{ mL min}^{-1}$ , and  $200 \text{ mL min}^{-1}$ , respectively; and the deposition time was 30 h.

The isothermal oxidation and thermal shock test of the coated sample was carried out at  $1400^\circ\text{C}$  in an electrical furnace. The furnace was first heated to  $1400^\circ\text{C}$  in air. After the temperature was steady, the coated sample was placed into the furnace and maintained at that temperature for a specified time. Meanwhile, the coated specimen was also subjected to thermal shock from  $1400^\circ\text{C}$  to room temperature when it was taken out of the furnace directly to air. Cumulative weight changes of the coated sample after every thermal cycle were measured by the precision balance and reported as a function of time. The surface and cross-section morphologies of the coating were observed with scanning electron microscopy (SEM). X-ray diffraction (XRD) and energy dispersive spectroscopy (EDS) were also used to identify crystalline structures and analyze element distribution in the coating, respectively.

### 3. Results and discussion

Fig. 1 shows the surface morphology, EDS and XRD analyses of the CVR SiC coating obtained on C/C composites. Fig. 1a is the typical surface morphology of

the prepared SiC coating, obviously, the coating is composed of many crystals together with large grains which are homogeneously distributed and randomly oriented. Though the piled up crystals form a “relatively dense structure”, however, cracks and holes are visible on the coating surface, which is unfavorable for the anti-oxidation property of the coating. Meanwhile, it should be noted that most of these formed crystals are revealed as well-developed hexagonal morphology, and the size of them is in the range from a few microns to one hundred microns. By EDS analysis (Fig. 1b), it can be verified that these crystals are composed of Si and C and the molar ratio of Si to C is close to one, indicating that the phase composition of the crystal is  $\beta$ -SiC. Fig. 1c shows an XRD scan of the as-prepared coating and it can be seen that there are only diffraction peaks for  $\beta$ -SiC, which further confirms that the phase composition of the inner coating is  $\beta$ -SiC.

Fig. 2 shows SEM images, EDS and XRD analyses of the outer layer CVD SiC coating. It is clear that the CVD outer coating displayed in Fig. 2a shows a smooth and dense surface morphology, and like the SiC inner coating, the CVD outer coating also consists of many piled up spherical particles in micron size. However, at high magnification, it is very interesting to find that the

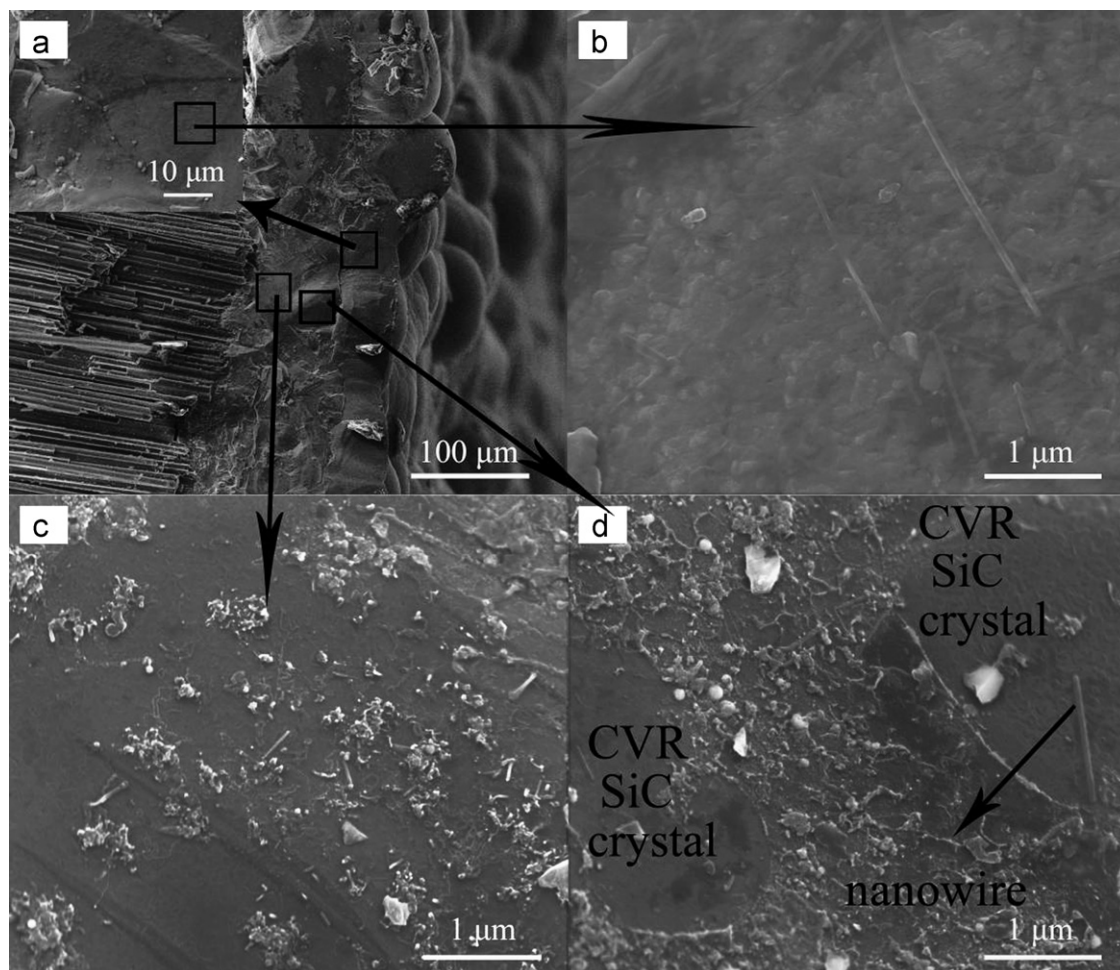


Fig. 3. Cross-section morphologies of the double layer nanostructure SiC coating prepared by CVR and CVD.

spherical particles in Fig. 2a are composed of the smaller polygonal particles which are stacked closely with each other. Fig. 2b shows the surface morphology of the polygonal particles with higher magnification. As shown in Fig. 2b, it is obvious that the coating is composed of many nanocrystals, meanwhile, the EDS analyses demonstrate that these crystals are SiC (Fig. 2c). Fig. 2d presents the XRD pattern of the CVD outer layer, the phase analysis result indicates that all the strong intensity peaks of the coating ( $2\theta=35.8^\circ$ ,  $59.9^\circ$ ,  $71.8^\circ$ ,  $75.2^\circ$ ) can be indexed as SiC (111), (220), (311) and (222) planes according to the JCPDS card No. 65–0360. Furthermore, compared with XRD pattern of the CVR SiC coating (Fig. 1c), the spectrum of the CVD SiC coating reveals an obvious broadening of the XRD peaks, and by using Scherrer formula, the average crystallite size of the SiC phase is calculated to be 14.5 nm, which is consistent with the SEM observation (Fig. 2b).

Fig. 3 shows the cross-section morphologies of the double layer nanostructure SiC coating prepared by CVR and CVD. Fig. 3a is the typical cross-section morphology of the double layer coating, as observed in Fig. 3a, the coating reveals a uniform thickness distribution and the thickness of the coating is over 120  $\mu\text{m}$ . Compared with SiC coatings prepared by other methods, this coating shows a special crystalline structure with limited porosity and also no distinct interface between the coating and the substrate, indicating the good compatibility and adherence between them. Further observation demonstrates that the CVD outer layer is rather dense, as the higher magnification micrograph showed in Fig. 3b. Interestingly, the outer dense CVD layer is composed primarily of SiC nanocrystals and nanowires. Furthermore, it should be mentioned that there are also many nanowires formed in the CVR inner layer (Fig. 3c), the formation of this dense inner layer with many nanowires may be explained as follows: because the inner CVR coating is not totally dense, and the pores or gaps existed in the coating are easy to absorb the deposition groups in the CVD process, after the deposition process, many SiC nanocrystals and nanowires are formed in the inner layer. Fig. 3d displays the typical surface morphology of the inner layer, from Fig. 3d, it's evident that the inner layer consists of many SiC microcrystals, nanocrystals and nanowires. As expected, SiC nanocrystals and nanowires are found around the large SiC crystals and together they formed a nearly dense structure.

Fig. 4 presents the isothermal oxidation curve of the double layer nanostructure SiC coating in air at 1400  $^\circ\text{C}$ . For a comparison, the oxidation behavior of the CVR SiC coated sample was also tested and the result shows that: just with 1 h oxidation, the weight loss of the coated sample is up to 1.72%. Compared with the single layer CVR SiC coating, the anti-oxidation property of the double layer nanostructure coating was improved significantly. After 400 h oxidation and 34 thermal cycles from 1400  $^\circ\text{C}$  to room temperature, the weight loss of the coated

sample is only 1.67%, which confirms that the prepared coating has excellent anti-oxidation property and thermal shock resistance at high temperature and it can provide

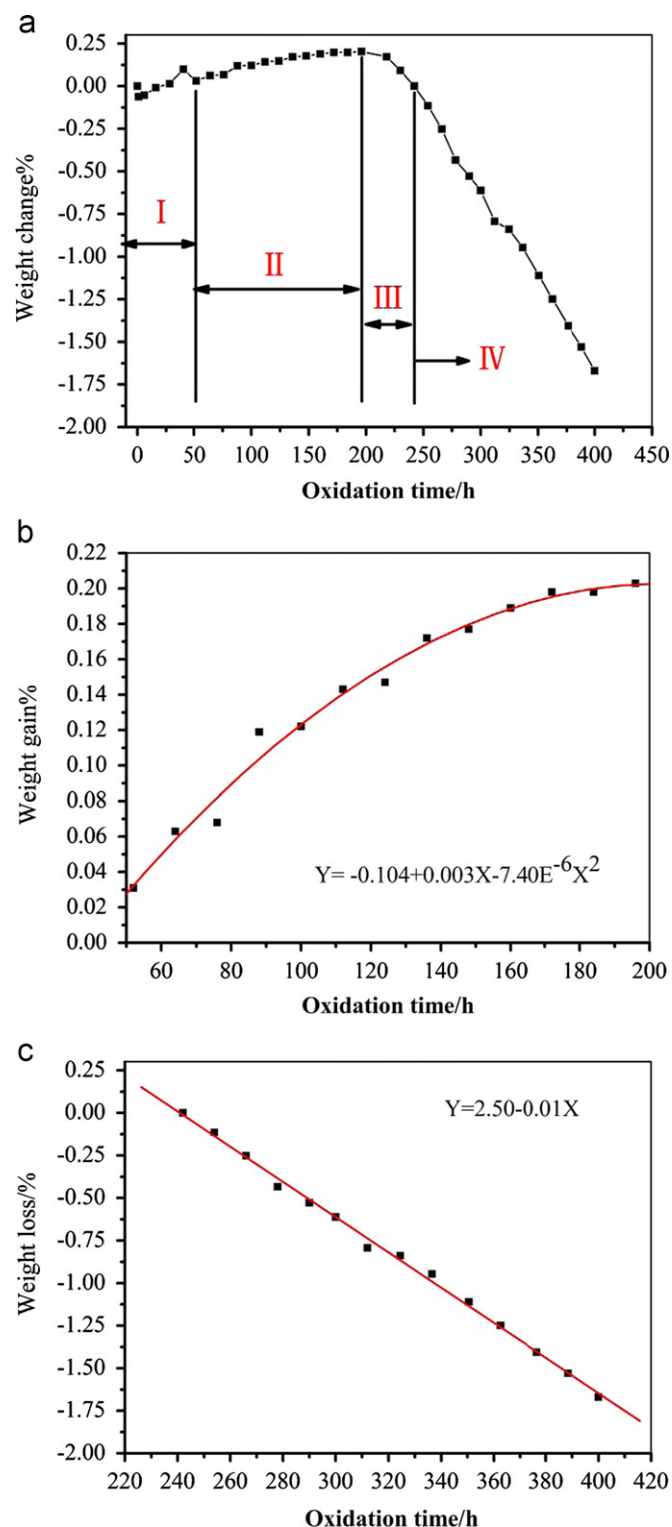


Fig. 4. Isothermal oxidation curves of the double layer nanostructure SiC coating in air at 1400  $^\circ\text{C}$ : (a) original isothermal oxidation curve of the coated sample in air at 1400  $^\circ\text{C}$ ; (b) the fitting results of weight gain curve in the oxidation process; (c) the fitting results of weight loss curve in the oxidation process.



long-term protection for C/C composites. Meanwhile, as shown in Fig. 4a, it can be seen that the whole oxidation curve of the coated sample can be divided into four stages: the self-healing stage (Fig. 4a–I), the weight gain stage (Fig. 4a–II), the transition stage (Fig. 4a–III) and the weight loss stage (Fig. 4a–IV). In the self-healing stage, the coated sample shows an unstable weight loss and weight gain course. While in the following stage, the coated sample gains weight continuously. As the oxidation and cyclic thermal shock test persisted, the coated sample begins to lose weight gradually. Moreover, the fitting results displayed in Fig. 4b and c show that the weight gain curve and weight loss curve in the oxidation process follow a typical parabolic and linear law, respectively, which are consistent with the reported oxidation kinetics of SiC coatings or ceramics [5,34–37].

Fig. 5 shows the surface morphologies of the double layer nanostructure SiC coating after oxidation in air at 1400 °C for different hours. From Fig. 5, it can be seen that the oxidized coating reveals a smooth and dense surface morphology. As oxidation time increased, the original spherical particles on the coating surface gradually vanished, and after 400 h oxidation, a smooth glass layer uniformly covered on the coating surface. Because the

formed SiO<sub>2</sub> glass has very low oxygen permeability and it can effectively flow and seal the defects on the coating surface, which enables the coating to have excellent anti-oxidation property and thermal shock resistance. Compared with other studies [3,5,21–23], it should be noted that no bubbles are formed on the coating surface as the surface morphologies showed in Fig. 5. Meanwhile, surface images with higher magnification further demonstrate that no bubbles are observed on the formed SiO<sub>2</sub> glass in the whole oxidation process (Fig. 6). According to the previous study [38], the bubble formation of the SiC coating in the oxidation process depends not only on oxidation temperature and pressure, but also on structural character such as the remaining defects in the coating or thickness of the layer. In the previous studies [3,5,21–23], the bubbles mainly formed as oxidation temperature exceeds 1500 °C. Consequently, it is reasonable to conclude that the relative low oxidation temperature and the dense structure of the coating may be the reason for no bubble formation in the oxidation process.

Moreover, according to the SEM images showed in Fig. 6, it is evident that the formed SiO<sub>2</sub> glass on the coating surface contains not only amorphous silica, but also some crystalline silica. It is well known that in passive

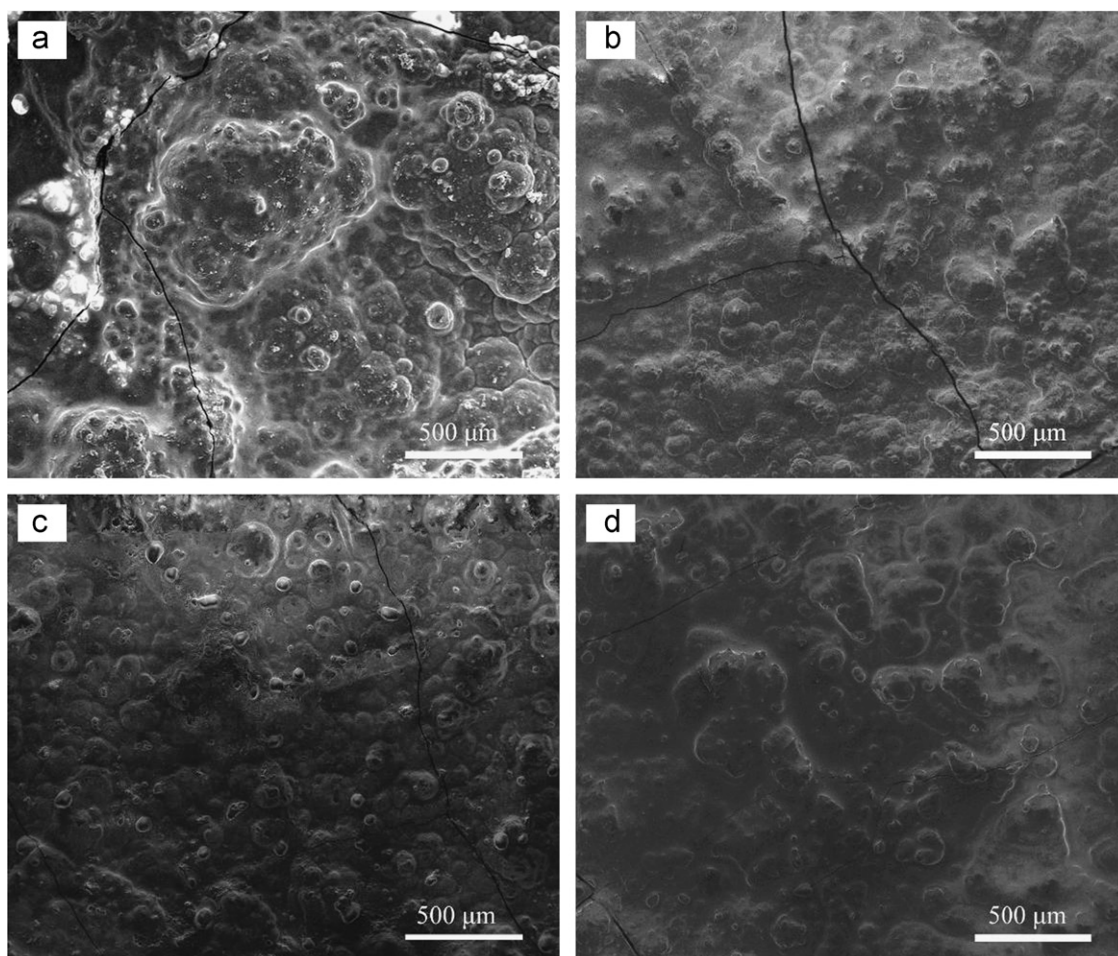


Fig. 5. SEM images of the double layer nanostructure SiC coating after oxidation in air at 1400 °C for different hours: (a) 76 h; (b) 160 h; (c) 300 h; (d) 400 h.

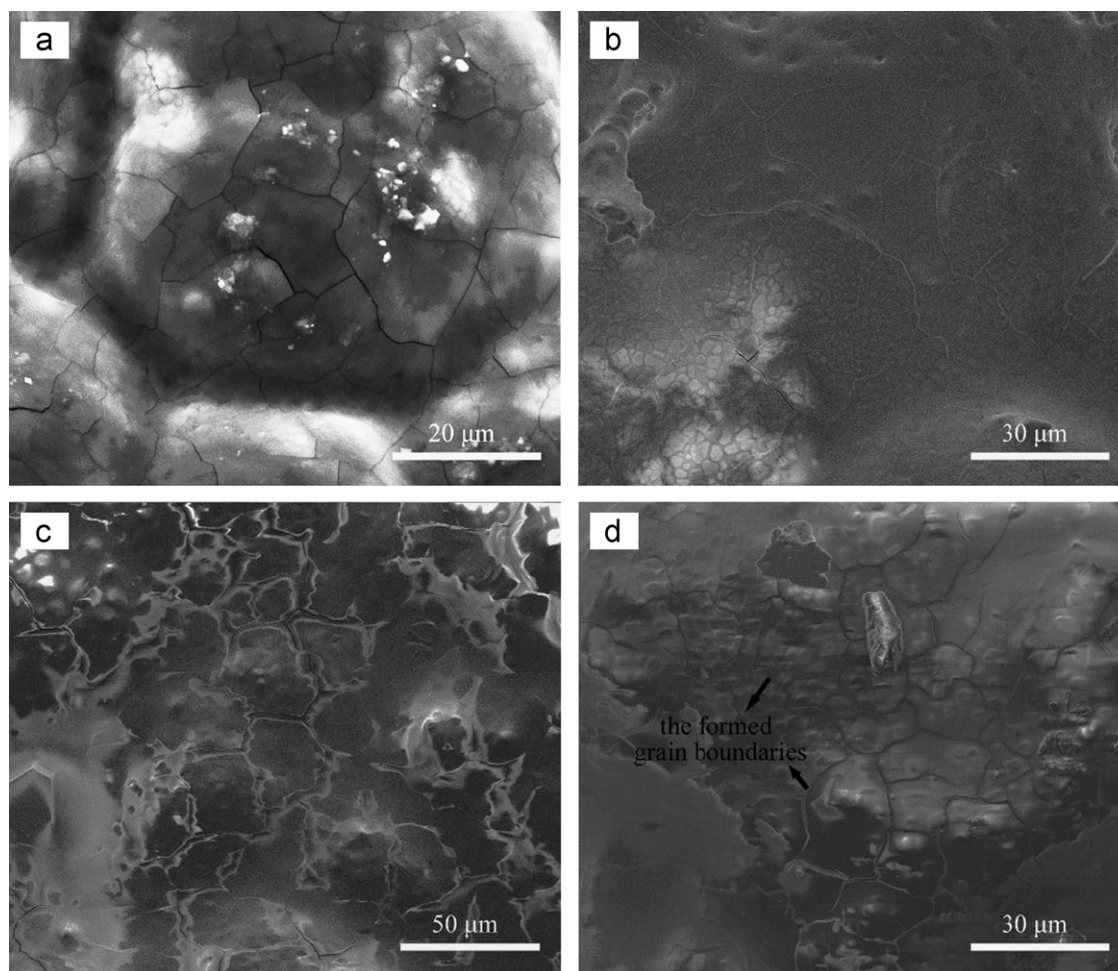


Fig. 6. Surface morphologies of the formed  $\text{SiO}_2$  glass on the SiC coating after oxidation in air at  $1400^\circ\text{C}$  for different hours: (a) 76 h; (b) 160 h; (c) 300 h; (d) clear grain boundaries are formed on  $\text{SiO}_2$  glass surface after 400 h oxidation.

oxidation, different kinds of silica such as amorphous silica and cristobalite may generate on SiC coating surface. However, as the oxidation time extended, amorphous silica formed at the beginning of the oxidation may crystallize to cristobalite at longer times and at high temperature [39,40]. As shown in Fig. 6, it is very interesting to find that clear grain boundary was formed on the  $\text{SiO}_2$  glass surface. To further understand the phase composition of the oxidized coating, the XRD analysis of the coating after different oxidation time was investigated and the results are displayed in Fig. 7. From Fig. 7, it is obvious that strong peaks corresponding to SiC and some weak peaks corresponding to cristobalite were detected in all spectra, indicating that the observed crystalline silica in Fig. 6 is cristobalite. The diffraction peaks at  $21.8^\circ$ ,  $28.3^\circ$ ,  $31.3^\circ$ ,  $44.7^\circ$ ,  $46.9^\circ$ ,  $48.5^\circ$  and  $54.0^\circ$  can be indexed as cristobalite (101), (111), (102), (202), (113), (212) and (203) planes, respectively, according to the JCPDS cards No. 39–1425. Particularly, it is noteworthy that the intensity peak of cristobalite (101) in the XRD patterns became stronger as oxidation time increased, which is consistent with previous studies [39,40]. Because the cristobalite has a larger CTE than the amorphous silica [41], the formation of the

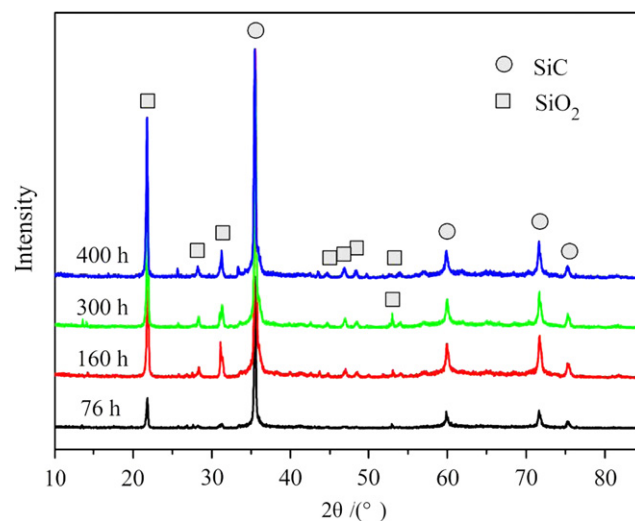


Fig. 7. XRD patterns of the double layer nanostructure SiC coating after oxidation in air at  $1400^\circ\text{C}$  for different hours: (a) 76 h; (b) 160 h; (c) 300 h; (d) 400 h.

cristobalite on the coating surface will increase the CTE mismatch and result in crack formation in the cyclic thermal shock test. Fig. 8 is the SEM images of the



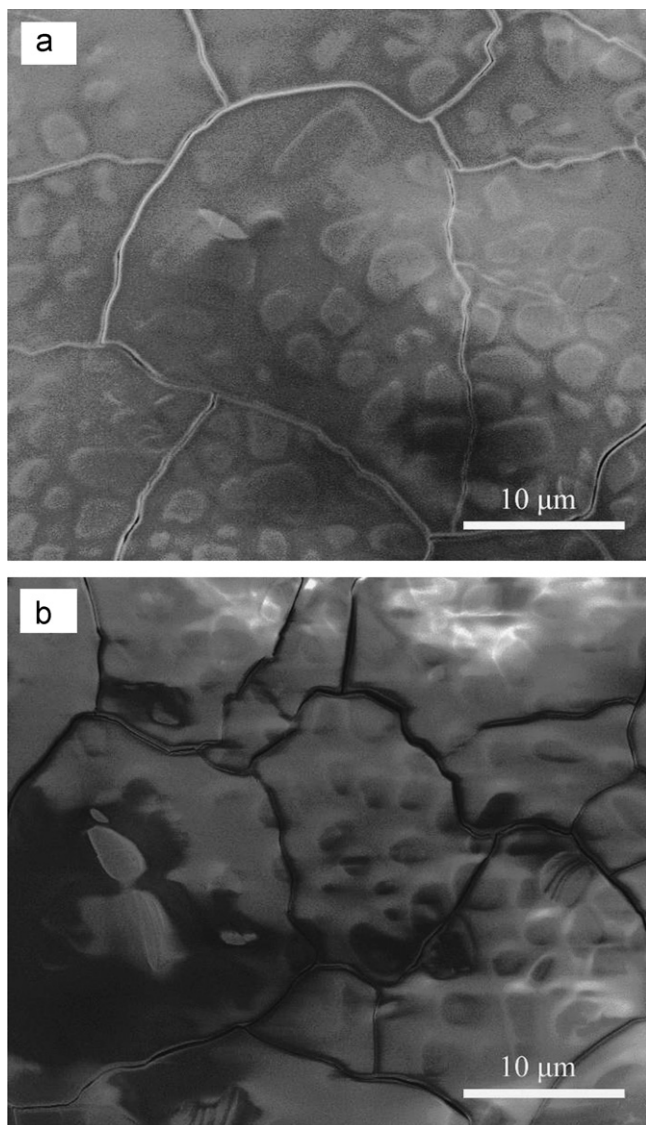


Fig. 8. SEM images of the micro-cracks formed along grain boundaries after oxidation and cyclic thermal shock test: (a) 160 h; (b) 400 h.

micro-cracks formed along grain boundaries after oxidation and cyclic thermal shock test. As shown in Fig. 8, it is clear that some micro-cracks were formed at or along the grain boundaries with increasing of oxidation time and thermal shock cycles, the formation of these cracks damages the stability of the  $\text{SiO}_2$  glass, which is unfavorable for the anti-oxidation property of the coating. Actually, with increasing of the thermal shock cycles and oxidation time, two types of cracks are formed. The first type of the crack presented in the silica layer is mainly correlated to formation of grain boundaries in thermal shock test, while the second type of the crack formed in the coating is associated with the thermal expansion mismatch between the coating and the substrate. Obviously, the formation of cracks in the silica layer damages the self-healing property of the silica glass at high temperature. In the following cyclic thermal shock test, the above two types of cracks may connect with each other and develop

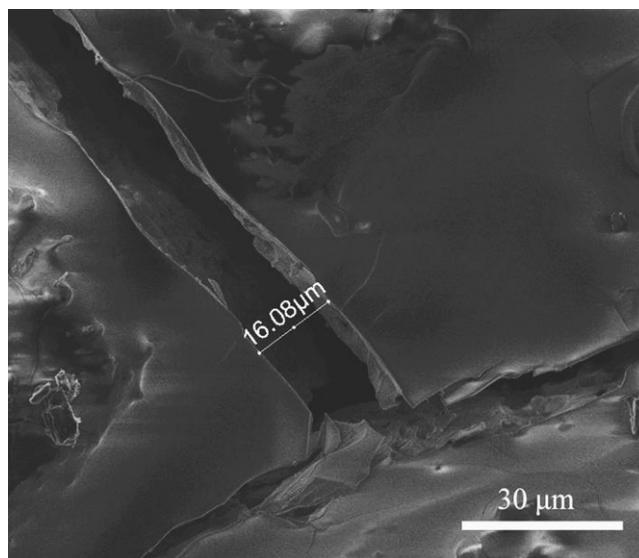


Fig. 9. Typical surface morphology of the cracks formed on the coating surface after 400 h oxidation and 34 cycles of thermal shock from 1400 °C to room temperature.

as penetration cracks. The formation of the penetration cracks offers the diffusion channel for oxygen to attack the substrate and results in weight loss of the coating. Fig. 9 shows the typical surface morphology of the cracks formed on the coating surface after 400 h oxidation and 34 cycles of thermal shock from 1400 °C to room temperature. From the above analysis, we can know that only cracks are formed on the coating surface, while other defects such as pores, bubbles or holes are not detected in the whole oxidation process, which may be attributed to the dense structure of the coating. Therefore, it can be concluded that the formation of the penetration cracks may be the reason for the weight loss of the SiC coated composite, though this aspect deserves further investigation. As is well known, the self-healing silica glass formed on the coating surface plays an important role in protecting C/C composites from oxidation. More specifically, the anti-oxidation property of the SiC coating is closely related to the stability of the formed silica glass. Therefore, to fully understand the correlation of the glass structure with the long-term anti-oxidation property of the SiC coating, systematic studies that focus on the phase transformation of the silica glass in long-term oxidation under a wide range of temperatures are our future work. Meanwhile, the defects evolution (cracks, bubbles and holes), especially the evolution of penetration defects accompanied in the above process should be investigated in detail.

#### 4. Conclusions

In summary, this paper reports a new double layer nanostructure SiC coating for anti-oxidation protection of C/C composites. This is the first time nanowires have been utilized in a double layer SiC coating for anti-oxidation purpose. The obtained dense coating reveals a typical



crystalline structure and combines well with the substrate. The inner layer of the coating was composed of SiC microcrystals, nanocrystals and nanowires, whereas the outer CVD layer mainly consists of SiC nanocrystals and nanowires. The obtained dense nanostructure coating shows excellent anti-oxidation behavior and thermal shock resistance at 1400 °C, after 400 h oxidation and 34 cycles of thermal shock from 1400 °C to room temperature, the weight loss of the coated sample is only 1.67%. As oxidation time and thermal shock cycles increased, the amorphous silica formed at the beginning of the oxidation crystallizes to cristobalite. Because the cristobalite has a larger CTE than the amorphous silica, the generation of the cristobalite resulted in micro-cracks formed along grain boundaries in the cyclic thermal shock test, which is unfavorable for the anti-oxidation property of the coating. In all, the accomplishment of this study may offer a new way to realize long-term protection for C/C composites applied in severe condition. Furthermore, as the CVR and CVD technology can both coated large complex components uniformly, the development of CVR and CVD method shows a potential advantage to extend C/C composites application in engineering and aerospace fields.

## Acknowledgments

This work has been supported by China Postdoctoral Science Foundation (2012M511752), the National 973 Program (2011CB605801), the Fundamental Research Funds for the Central Universities (2012QNZT004), the freedom explore program of Central South University and the Postdoctoral Science Foundation of Central South University.

## References

- [1] K.Z. Li, F.T. Lan, H.J. Li, X.T. Shen, Y.G. He, Oxidation protection of carbon/carbon composites with SiC/indialite coating for intermediate temperatures, *Journal of the European Ceramic Society* 29 (2009) 1803–1807.
- [2] F. Smeacetto, M. Salvo, M. Ferraris, Oxidation protective multilayer coatings for carbon–carbon composites, *Carbon* 40 (2002) 583–587.
- [3] Q.G. Fu, H.J. Li, X.H. Shi, K.Z. Li, G.D. Sun, Silicon carbide coating to protect carbon/carbon composites against oxidation, *Scripta Materialia* 52 (2005) 923–927.
- [4] S.J. Wu, L.F. Cheng, L.T. Zhang, Y.D. Xu, Oxidation behavior of 2D C/SiC with a multi-layer CVD SiC coating, *Surface and Coatings Technology* 200 (2006) 4489–4492.
- [5] J.F. Huang, X.R. Zeng, H.J. Li, X.B. Xiong, Y.W. Fu, Influence of the preparation temperature on the phase, microstructure and anti-oxidation property of a SiC coating for C/C composites, *Carbon* 42 (2004) 1517–1521.
- [6] L.F. Cheng, Y.D. Xu, L.T. Zhang, X.W. Yin, Preparation of an oxidation protection coating for C/C composites by low pressure chemical vapor deposition, *Carbon* 38 (2000) 1493–1498.
- [7] N.S. Jacobson, D.J. Roth, R.W. Rausser, J.D. Cawley, D.M. Curry, Oxidation through coating cracks of SiC-protected carbon/carbon, *Surface and Coatings Technology* 203 (2008) 372–383.
- [8] L. Snell, A. Nelson, P. Molian, A novel laser technique for oxidation-resistant coating of carbon–carbon composite, *Carbon* 39 (2001) 991–999.
- [9] R. Israel, G. Combarieu, B. Drevet, D. Camel, N. Eustathopoulos, O. Raymond, Resistance to oxidation of graphite silicided by reactive infiltration, *Journal of the European Ceramic Society* 31 (2011) 2167–2174.
- [10] J. Zhao, G. Wang, Q.G. Guo, L. Liu, Microstructure and property of SiC coating for carbon materials, *Fusion Engineering and Design* 82 (2007) 363–368.
- [11] C. Hu, Y.R. Niu, H. Li, M.S. Ren, X.B. Zheng, J.L. Sun, SiC coatings for carbon/carbon composites fabricated by vacuum plasma spraying technology, *Journal of Thermal Spray Technology* 21 (2012) 16–22.
- [12] F. Smeacetto, M. Ferraris, M. Salvo, Multilayer coating with self-sealing properties for carbon–carbon composites, *Carbon* 41 (2003) 2105–2111.
- [13] O.S. Kwon, S.H. Hong, H. Kim, The improvement in oxidation resistance of carbon by a graded SiC/SiO<sub>2</sub> coating, *Journal of the European Ceramic Society* 23 (2003) 3119–3124.
- [14] Z.Q. Yan, X. Xiong, P. Xiao, F. Chen, H.B. Zhang, B.Y. Huang, A multilayer coating of dense SiC alternated with porous Si–Mo for the oxidation protection of carbon/carbon silicon carbide composites, *Carbon* 46 (2008) 149–153.
- [15] X.H. Zheng, Y.G. Du, J.Y. Xiao, Y.F. Lu, C.Y. Liang, Celsian/yttrium silicate protective coating prepared by microwave sintering for C/SiC composites against oxidation, *Materials Science and Engineering A* 505 (2009) 187–190.
- [16] Y.C. Lin, E.M. Ruiz, R.G. Rateick Jr., P.J. McGinn, A.S. Mukasyan, One-step synthesis of a multi-functional anti-oxidation protective layer on the surface of carbon/carbon composites, *Carbon* 50 (2012) 557–565.
- [17] X.Y. Yao, H.J. Li, Y.L. Zhang, H. Wu, X.F. Qiang, A SiC–Si–ZrB<sub>2</sub> multiphase oxidation protective ceramic coating for SiC-coated carbon/carbon composites, *Ceramics International* 38 (2012) 2095–2100.
- [18] Y. Xiang, W. Li, S. Wang, Z.H. Chen, Oxidation behavior of oxidation protective coatings for PIP–C/SiC composites at 1500 °C, *Ceramics International* 38 (2012) 9–13.
- [19] C.A.A. Cairo, M.L.A. Graca, C.R.M. Silva, J.C. Bressiani, Functionally gradient ceramic coating for carbon–carbon antioxidation protection, *Journal of the European Ceramic Society* 21 (2001) 325–329.
- [20] J.I. Kim, W.J. Kim, D.J. Choi, J.Y. Park, W.S. Ryu, Design of a C/SiC functionally graded coating for the oxidation protection of C/C composites, *Carbon* 43 (2005) 1749–1757.
- [21] Y.L. Zhang, H.J. Li, Q.G. Fu, K.Z. Li, J. Wei, P.Y. Wang, A C/SiC gradient oxidation protective coating for carbon/carbon composites, *Surface and Coatings Technology* 201 (2006) 3491–3495.
- [22] H.J. Li, Q.G. Fu, X.H. Shi, K.Z. Li, Z.B. Hu, SiC whisker-toughened SiC oxidation protective coating for carbon/carbon composites, *Carbon* 44 (2006) 602–605.
- [23] Q.G. Fu, H.J. Li, Z.Z. Zhang, X.R. Zeng, K.Z. Li, SiC nanowire-toughened MoSi<sub>2</sub>–SiC coating to protect carbon/carbon composites against oxidation, *Corrosion Science* 52 (2010) 1879–1882.
- [24] G.B. Zheng, H. Mizuki, H. Sano, Y. Uchiyama, CNT–PyC–SiC/SiC double-layer oxidation-protection coating on C/C composite, *Carbon* 46 (2008) 1808–1811.
- [25] Y. Chen, C.G. Wang, W. Zhao, W.B. Lu, A.T. Chen, T.T. Tan, Fabrication of a SiC/Si/MoSi<sub>2</sub> multi-coating on graphite materials by a two-step technique, *Ceramics International* 38 (2012) 2165–2170.
- [26] Y.H. Chu, H.J. Li, Q.G. Fu, H.P. Wang, X.H. Hou, X. Zou, G.N. Shang, Oxidation protection of C/C composites with a multilayer coating of SiC and Si+SiC+SiC nanowires, *Carbon* 50 (2012) 1280–1288.
- [27] X.F. Qiang, H.J. Li, Y.L. Zhang, D.J. Yao, L.J. Guo, J.F. Wei, Fabrication and thermal shock resistance of in situ SiC nanowire–SiC/SiC coating for carbon/carbon composites, *Corrosion Science* 59 (2012) 343–347.

- [28] K.L. Choy, Chemical vapour deposition of coatings, *Progress in Materials Science* 48 (2003) 57–170.
- [29] W. Yang, H. Araki, Q. Hu, N. Ishikawa, H. Suzuki, T. Noda, In situ growth of SiC nanowires on RS-SiC substrate(s), *Journal of Crystal Growth* 264 (2004) 278–283.
- [30] W. Yang, H. Araki, S. Thaveethavorn, H. Suzuki, T. Noda, In situ synthesis and characterization of pure SiC nanowires on silicon wafer, *Applied Surface Science* 241 (2005) 236–240.
- [31] Q.G. Fu, H.J. Li, X.H. Shi, K.Z. Li, Z.B. Hu, J. Wei, Microstructure and growth mechanism of SiC whiskers on carbon/carbon composites prepared by CVD, *Materials Letters* 59 (2005) 2593–2597.
- [32] W. Kowbel, J.C. Withers, P.O. Ransone, CVD and CVR silicon-based functionally gradient coatings on C–C composites, *Carbon* 33 (1995) 415–426.
- [33] X. Yang, Q.Z. Huang, Y.H. Zou, X. Chang, Z.A. Su, M.Y. Zhang, Z.Y. Xie, Anti-oxidation behavior of chemical vapor reaction SiC coatings on different carbon materials at high temperatures, *Transactions of Nonferrous Metals Society of China* 19 (2009) 1044–1050.
- [34] J. Li, R.Y. Luo, Y.P. Chen, Q. Xiang, C. Lin, P. Ding, N. An, J.W. Cheng, Oxidation behavior and kinetics of SiC/alumina–borosilicate coating for carbon-carbon composites, *Applied Surface Science* 255 (2008) 1967–1974.
- [35] J.A. Costello, R.E. Tressler, Oxidation kinetics of silicon carbide crystals and ceramics. I, in dry oxygen, *Journal of the American Ceramic Society* 69 (1986) 674–681.
- [36] M. Villegas, T. Sierra, F. Lucas, J.F. Fernández, A.C. Caballero, Oxidation treatments for SiC particles and its compatibility with glass, *Journal of the European Ceramic Society* 27 (2007) 861–865.
- [37] X.M. Hou, K.C. Chou, F.S. Li, A new treatment for kinetics of oxidation of silicon carbide, *Ceramics International* 35 (2009) 603–607.
- [38] M. Auweter-kurtz, G. Hilfer, H. Habiger, K. Yamawaki, T. Yoshinaka, H.D. Speckmann, Investigation of oxidation protected C/C heat shield material in different plasma wind tunnels, *Acta Astronautica* 45 (1999) 93–108.
- [39] X.M. Hou, K.C. Chou, Model of oxidation of SiC microparticles at high temperature, *Corrosion Science* 50 (2008) 2367–2371.
- [40] Q.S. Zhu, X.L. Qiu, C.W. Ma, The oxidation resistance improvement of matrix graphite of spherical fuel elements by slip-gelation process, *Journal of Nuclear Materials* 254 (1998) 221–225.
- [41] K. Toshiki, T. Masaharu, Y. Toshio, I. Kenjiro, M. Hiroki, Correlation between the oxidation behavior and the microstructure of SiC coatings deposited on graphite substrates via chemical vapor deposition, *Thin Solid Films* 315 (1998) 139–143.